

Fluorescent Protein-Based Turn-On Probe Through A General Protection-Deprotection Design Strategy

Xin Shang,¹ Nanxi Wang, Ronald Cerny, Wei Niu,² Jiantao Guo^{1*}

1. Department of Chemistry, University of Nebraska-Lincoln, Lincoln, Nebraska, 68588, United States.

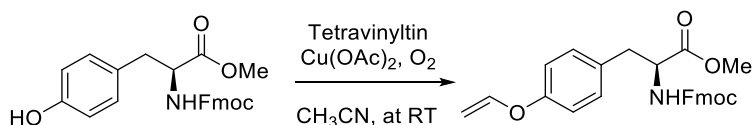
2. Department of Chemical & Biomolecular Engineering, University of Nebraska-Lincoln, Lincoln, Nebraska, 68588, United States.

Supporting Information

I. Synthetic procedures.....	S-3
II. Primer list.....	S-4
III. Supplemental figures and tables	
1. Figure S1.....	S-5
2. Figure S2.....	S-6
3. Figure S3.....	S-7
4. Figure S4.....	S-8
5. Figure S5.....	S-9
6. Figure S6.....	S-10
7. Figure S7.....	S-11
8. Figure S8.....	S-12
9. Figure S9.....	S-13
10. Figure S10.....	S-14
11. Figure S11.....	S-15
12. Figure S12.....	S-16
13. Figure S13.....	S-17
14. Table S1.....	S-18
IV. References.....	S-23

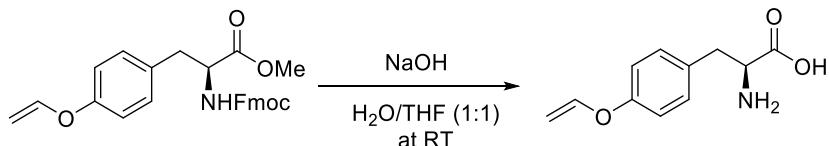
I. Synthetic procedures

N-(9-Fluorenylmethoxycarbonyl)-*p*-vinyloxy-L-phenylalanine methyl ester



Anhydrous $\text{Cu}(\text{OAc})_2$ (220 mg, 1.2 mmol) was added to a solution of *N*-(9-Fluorenylmethoxycarbonyl)-L-tyrosine methyl ester¹ (417 mg, 1.0 mmol) in 5 mL of acetonitrile. The mixture was bubbled with oxygen for half an hour and then tetravinyltin (220 μL , 1.2 mmol) was added with stirring. After being stirred at room temperature for 22 hours, the reaction mixture was poured into 30 mL of 25% aqueous solution of ammonium acetate. The resulting solution was extracted with ethyl acetate (30 mL \times 3). The combined organic layers were washed with brine, dried over sodium sulfate, and concentrated under vacuum. The residue was further purified by silica gel flash chromatography (hexane/ethyl acetate, from 20/1 to 4/1, v/v). Desired product (359 mg) was obtained as white solid. The yield was 81%. $^1\text{H-NMR}$ (400 MHz, CDCl_3 ; Figure S8) δ ppm: 7.77 (d, J = 7.5 Hz, 2H), 7.57 (t, J = 6.3 Hz, 2H), 7.45 – 7.36 (m, 2H), 7.32 (tt, J = 7.5, 1.4 Hz, 2H), 7.03 (d, J = 8.2 Hz, 2H), 6.92 (d, J = 8.5 Hz, 2H), 6.60 (dd, J = 13.7, 6.0 Hz, 1H), 5.23 (d, J = 8.2 Hz, 1H), 4.76 (dd, J = 13.7, 1.7 Hz, 1H), 4.64 (m, 1H), 4.50 – 4.45 (m, 1H), 4.43 (m, 1H), 4.36 (m, 1H), 4.21 (t, J = 6.9 Hz, 1H), 3.73 (s, 3H), 3.08 (m, 2H). $^{13}\text{C-NMR}$ (101 MHz, CDCl_3) δ ppm: 171.99, 156.09, 155.65, 148.18, 143.97, 143.84, 141.48, 130.65, 127.88, 127.21, 125.21, 125.15, 120.15, 120.13, 117.30, 95.40, 77.48, 77.16, 76.84, 67.04, 54.95, 52.53, 47.33, 37.62. MS (ESI) calcd for $\text{C}_{27}\text{H}_{25}\text{NO}_5$, $[\text{M} + \text{H}]^+$ 444.2, found 443.7.

***p*-vinyloxy-L-phenylalanine (ViP)**



The purified product from the above step was dissolved in 2.25 mL of tetrahydrofuran (THF), followed by dropwise addition of the same volume of 1 N aqueous solution of sodium hydroxide with stirring. After being stirred at room temperature for 24 hours, the mixture was washed with diethyl ether multiple times until no byproduct in the organic layer was detected by TLC. The aqueous layer was diluted and neutralized. The resulting solution was desalinated by Amberlite

XAD4 flash chromatography, affording 55 mg yellowish product (yield: 59%). ¹H-NMR (400MHz, D₂O; Figure S9) δ ppm: 7.31 (d, *J* = 8.6 Hz, 2H), 7.10 (d, *J* = 8.6 Hz, 2H), 6.79 (dd, *J* = 13.7, 6.1 Hz, 1H), 4.82 (dd, *J* = 13.7, 1.9 Hz, 1H), 4.56 (dd, *J* = 6.1, 1.9 Hz, 1H), 3.97 (dd, *J* = 7.8, 5.3 Hz, 1H), 3.25 (dd, *J* = 14.6, 5.3 Hz, 1H), 3.11 (dd, *J* = 14.6, 7.8 Hz, 1H). ¹³C-NMR (101 MHz, D₂O) δ ppm: 182.38, 154.93, 148.64, 133.42, 130.81, 117.19, 94.90, 57.65, 40.08. MS (ESI) calcd for C₁₁H₁₃NO₃, [M + H]⁺ 208.1, found 208.3

II Primer list

P1: 5'-GAGGAGAAATTACATATGTCCAAG-3'

P2: 5'- AGTGAGGGTAGTTACCAGGGT-3'

P3: 5'-ACCCTGGTAACTACCCCTCACTtatGGTGTCCAGTGCTTCTCTCG-3'

P4: 5'-GAGTCCAAGCTCAGCGGTG-3'

P5: 5'-GTGGCTATTGAAGTTACTCCA-3'

P6: 5'-TGGAGTATAACTCAATAGCCACtagGTGTACATCACTGCTGATAAACAG-3'

III. Supplemental figures

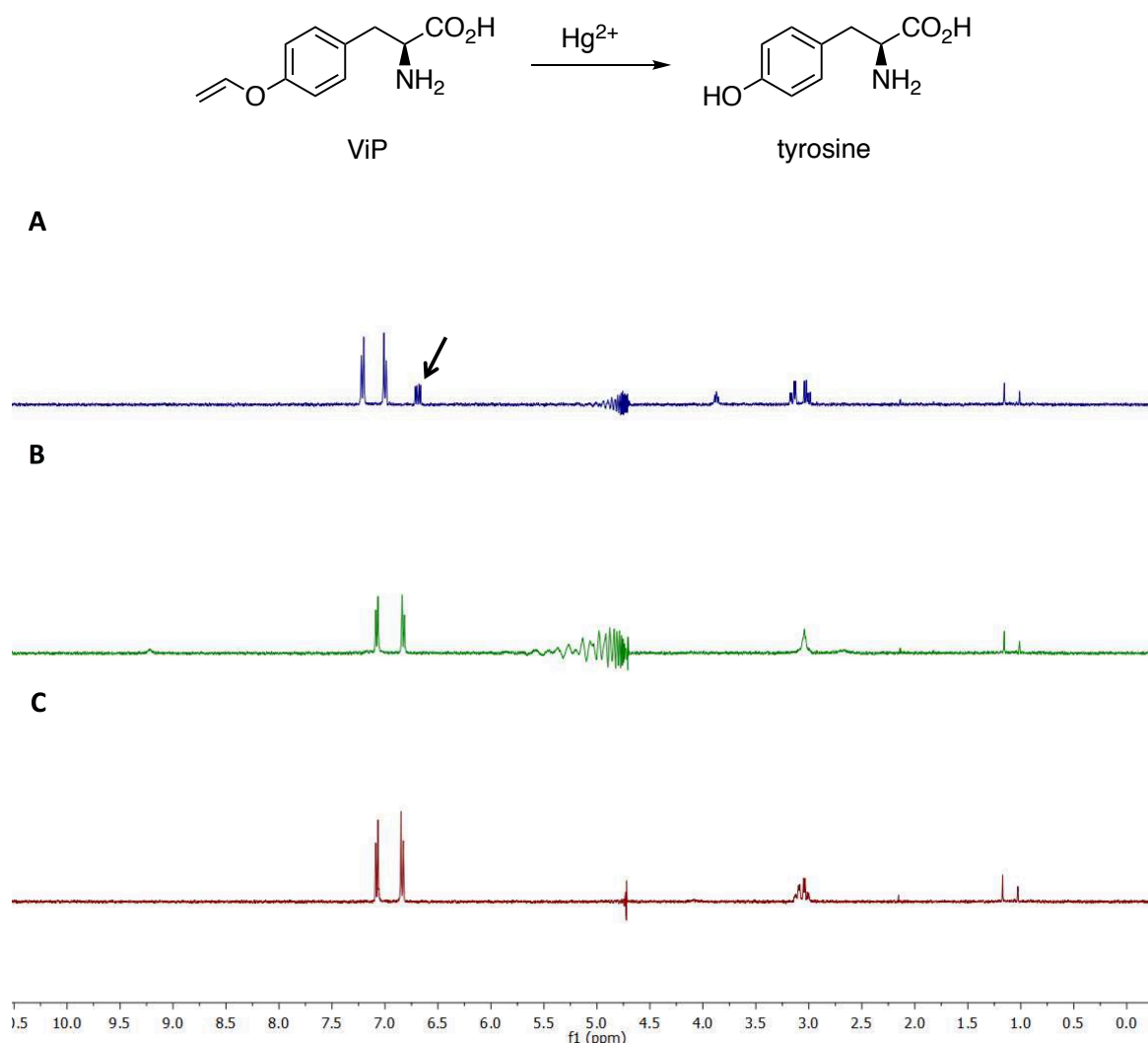


Figure S1. Water suppression NMR study of the deprotection of ViP with Hg^{2+} . (A) NMR spectrum of ViP (2 mM) in the absence of Hg^{2+} . The proton of the vinyloxy group next to the oxygen was observed at δ 6.8 ppm (arrow). The signal from other two protons of the vinyloxy group were suppressed due to their proximity to the water peak; (B) NMR spectrum of ViP (2 mM) in the presence of 2 mM Hg^{2+} . The NMR spectrum was taken immediately after the addition of Hg^{2+} ; (C) NMR spectrum of tyrosine (2 mM).

The deprotection product was confirmed to be tyrosine.

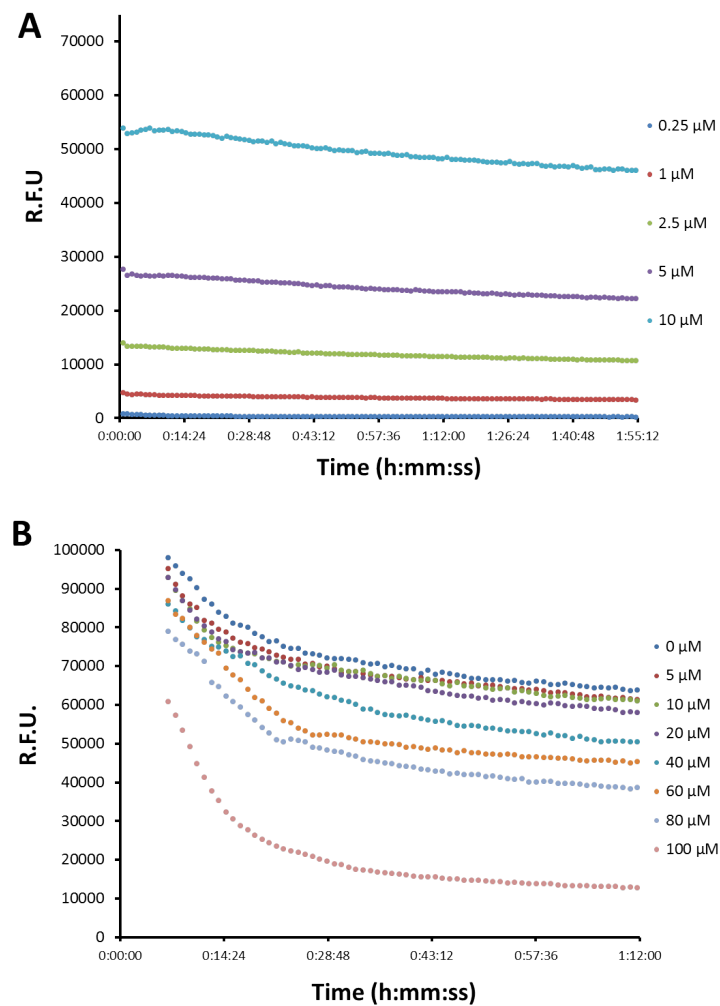


Figure S2. Time courses of the fluorescence intensity changes of wild-type sfGFP in the presence of Hg^{2+} . (A) Varied concentrations of wild-type sfGFP were incubated with 100 μM Hg^{2+} ; (B) The wild-type sfGFP (0.25 μM) was incubated with varied concentrations of Hg^{2+} . The reduced fluorescence intensity over time is likely due to the bleaching of the FP.

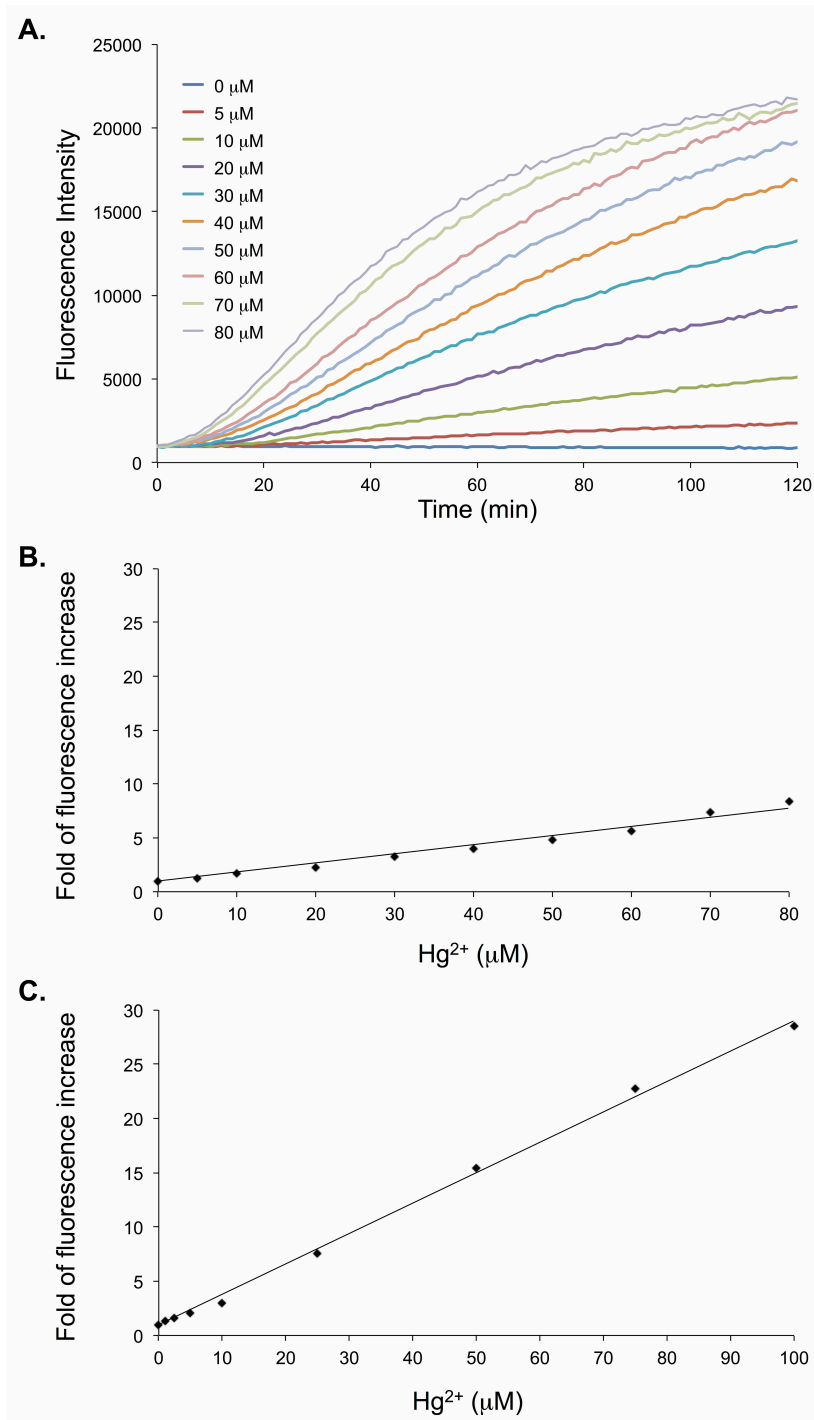


Figure S3. Hg²⁺ Sensing using sfGFP variants. (A) Time courses of fluorescence intensity change of sfGFP-Tyr66ViP in the presence of varied concentrations of Hg²⁺; (B) Changes in fluorescence of sfGFP-Tyr66ViP after an incubation with different concentrations of Hg²⁺ for 30 min; (C) Changes in fluorescence of cpsfGFP-Tyr66ViP after an incubation with different concentrations of Hg²⁺ for 30 min.

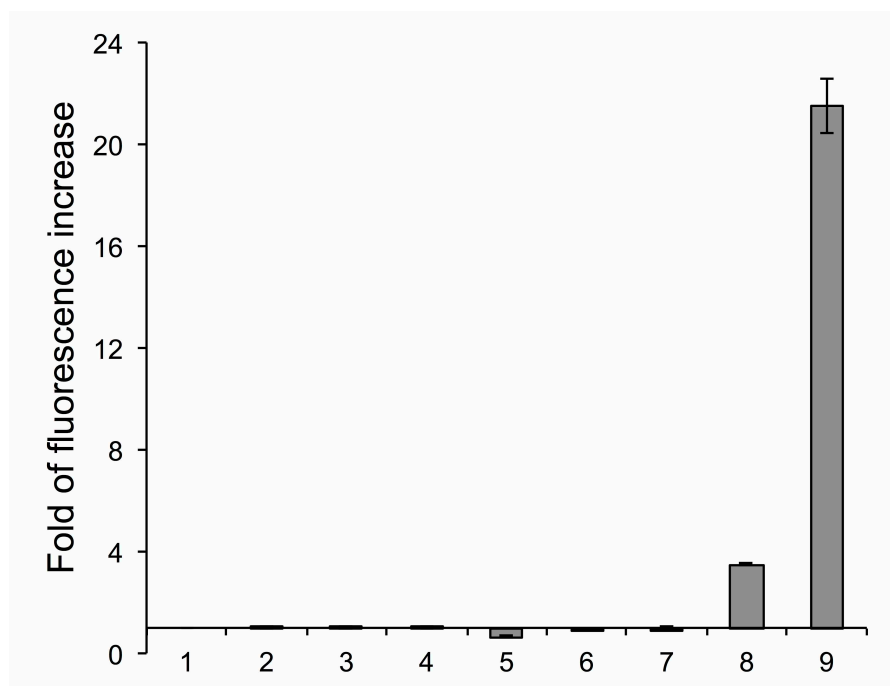


Figure S4. Fluorescence changes of sfGFP-Tyr66ViP (0.5 μ M) in response to different metal ions after 90 minutes of incubation. 1, blank (no metal ion added); 2, 100 μ M Zn²⁺; 3, 100 μ M Mg²⁺; 4, 100 μ M Mn²⁺; 5, 100 μ M Cu²⁺; 6, 100 μ M Co²⁺; 7, 100 μ M Ca²⁺; 8, 10 μ M Hg²⁺; 9, 100 μ M Hg²⁺.

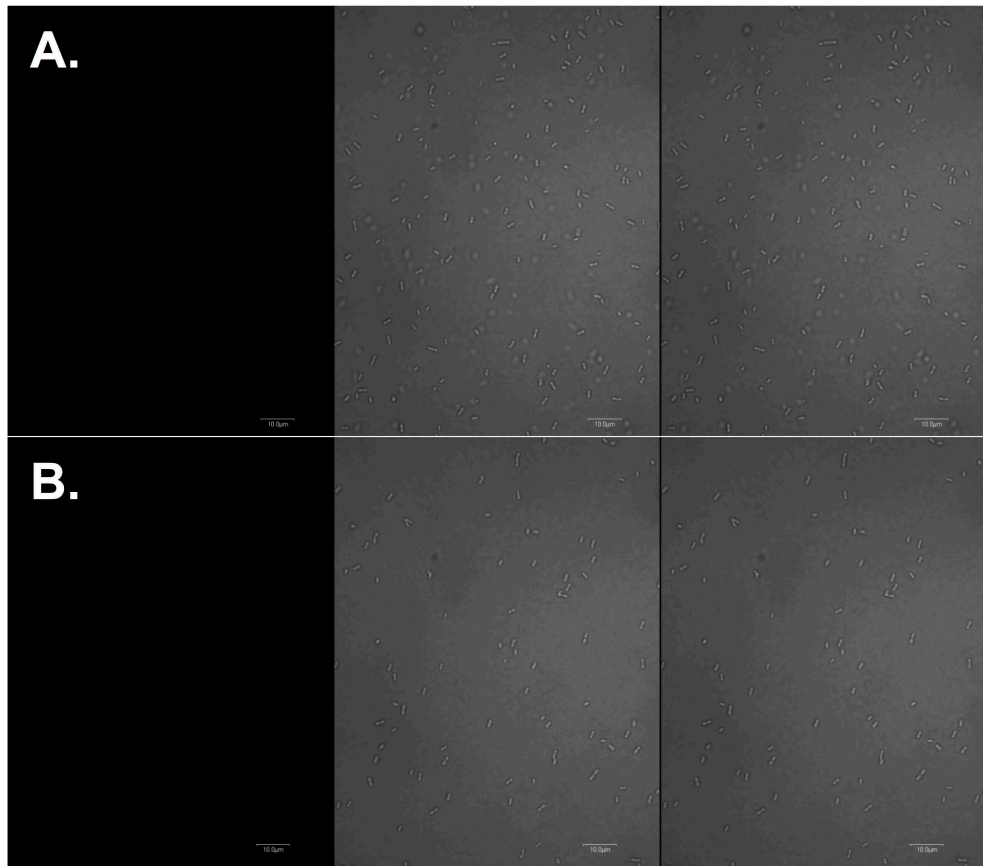


Figure S5. Fluorescence imaging of live *E. coli* cells expressing sfGFP variants. (A) *E. coli* cells expressing sfGFP-Tyr66TAG in the absence of ViP, after the addition of Hg²⁺; (B) *E. coli* cells expressing sfGFP-Tyr66TAG in the absence of PrFRS, after the addition of Hg²⁺. For all images, the left panel shows fluorescent images of *E. coli* cells in FITC channel (494 nm excitation and 518 nm emission), the middle panel shows bright-field images of the same *E. coli* cells, and the right panel shows composite images of bright-field and fluorescent images. Scale bars, 10 μ m.

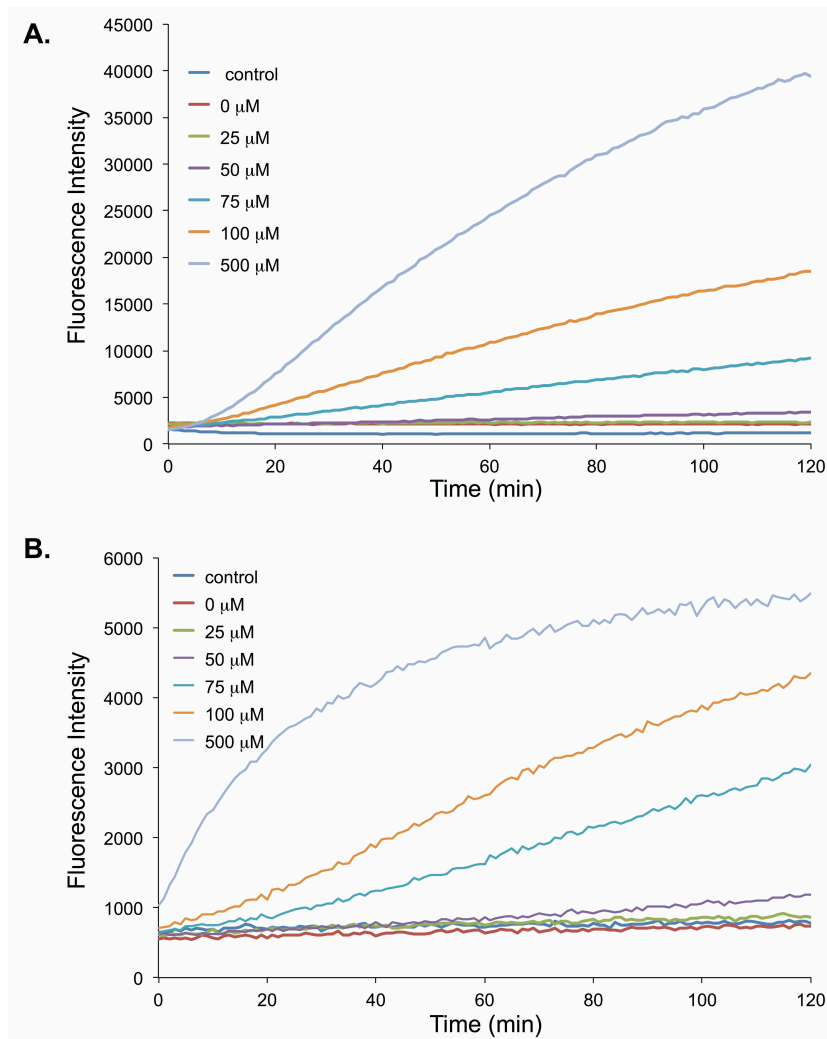


Figure S6. Time courses of fluorescence intensity change of cells expressing sfGFP-Tyr66ViP or cpsfGFP-Tyr66ViP in the presence of Hg^{2+} . (A) sfGFP-Tyr66ViP in the presence of different concentrations of Hg^{2+} at varying time points; (B) cpsfGFP-Tyr66ViP in the presence of different concentrations of Hg^{2+} for 5 h.

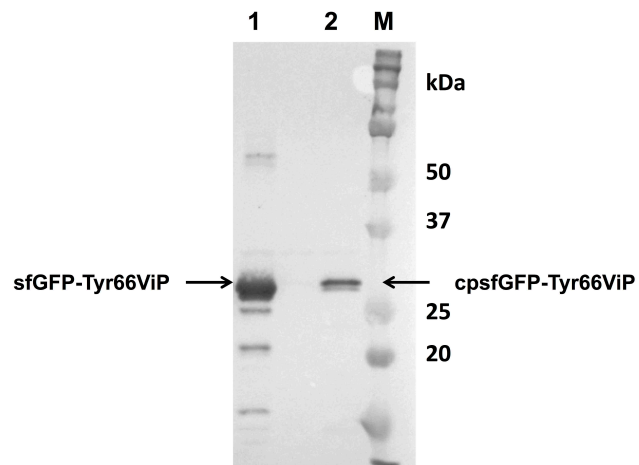


Figure S7. Protein expression levels of sfGFP-Tyr66ViP and cpsfGFP-Tyr66ViP. The protein expression level was detected by Western blot using anti-His₆ tag antibody. The same amount of cells was used in this analysis. Lane 1, sfGFP-Tyr66ViP; Lane 2, cpsfGFP-Tyr66ViP; lane M, molecular weight marker.

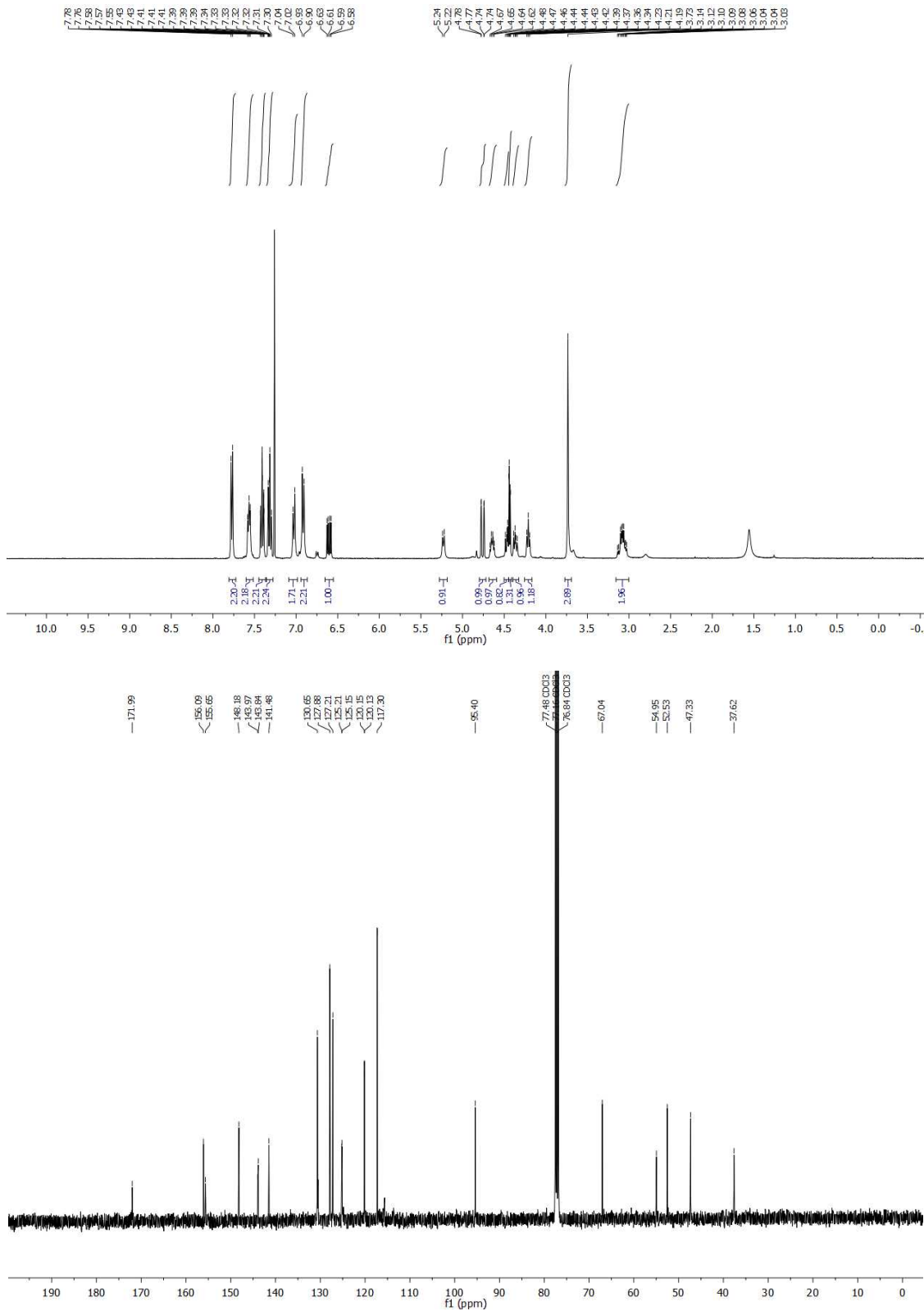


Figure S8. ^1H and ^{13}C NMR spectra of *N*-(9-fluorenylmethoxycarbonyl)-*p*-vinyloxy-L-phenylalanine methyl ester.

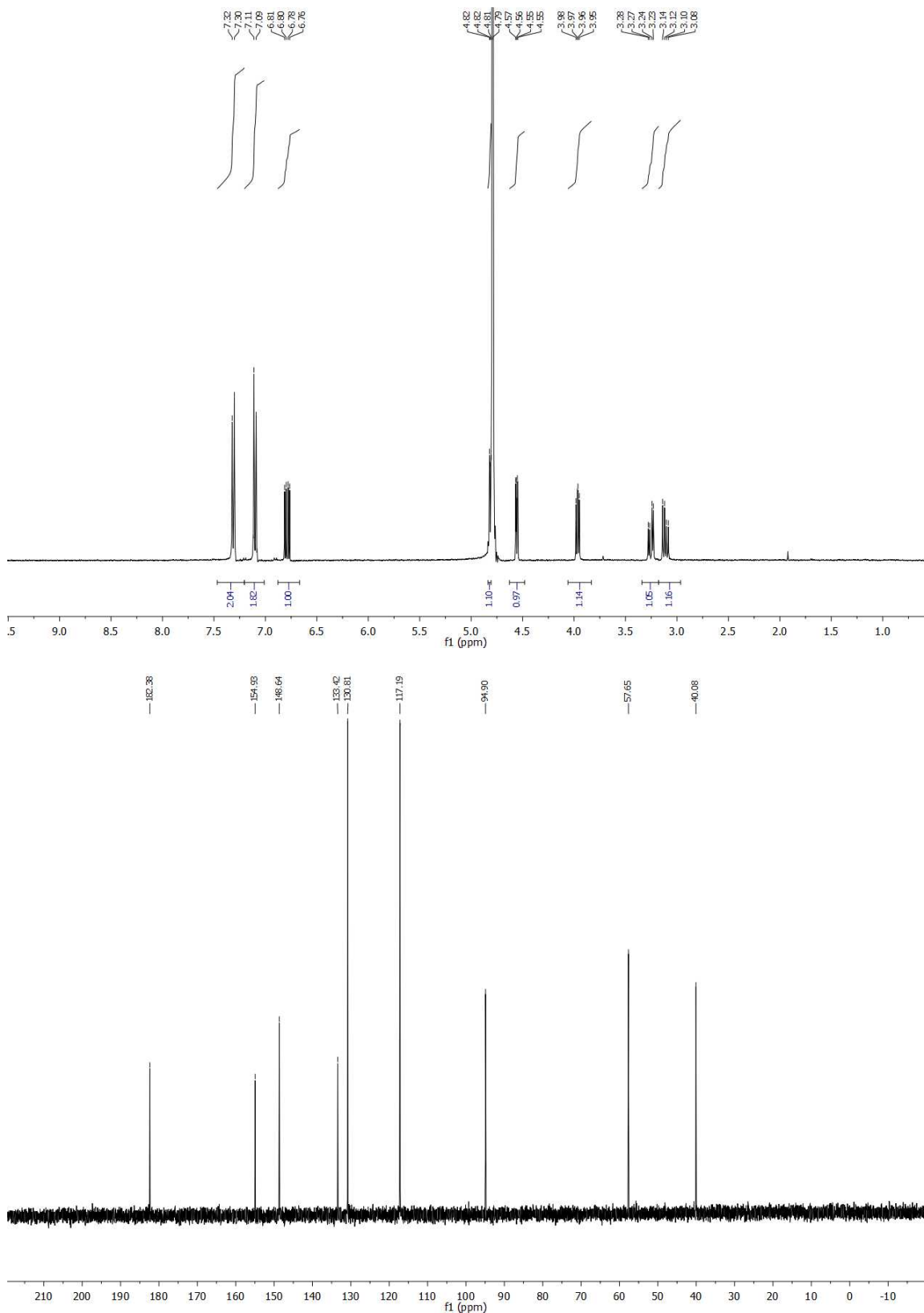


Figure S9. ¹H and ¹³C NMR spectra of ViP.

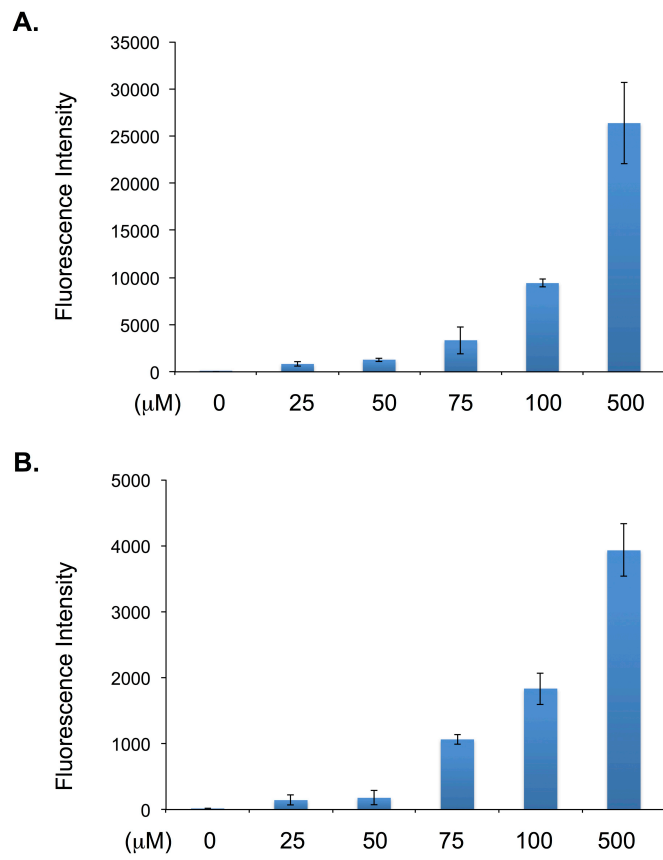


Figure S10. Fluorescence intensity change of cells expressing sfGFP-Tyr66ViP or cpsfGFP-Tyr66ViP in the presence of different concentrations of Hg^{2+} . (A) sfGFP-Tyr66ViP in the presence of different concentrations of Hg^{2+} for 1 h; (B) cpsfGFP-Tyr66ViP in the presence of different concentrations of Hg^{2+} for 1 h.

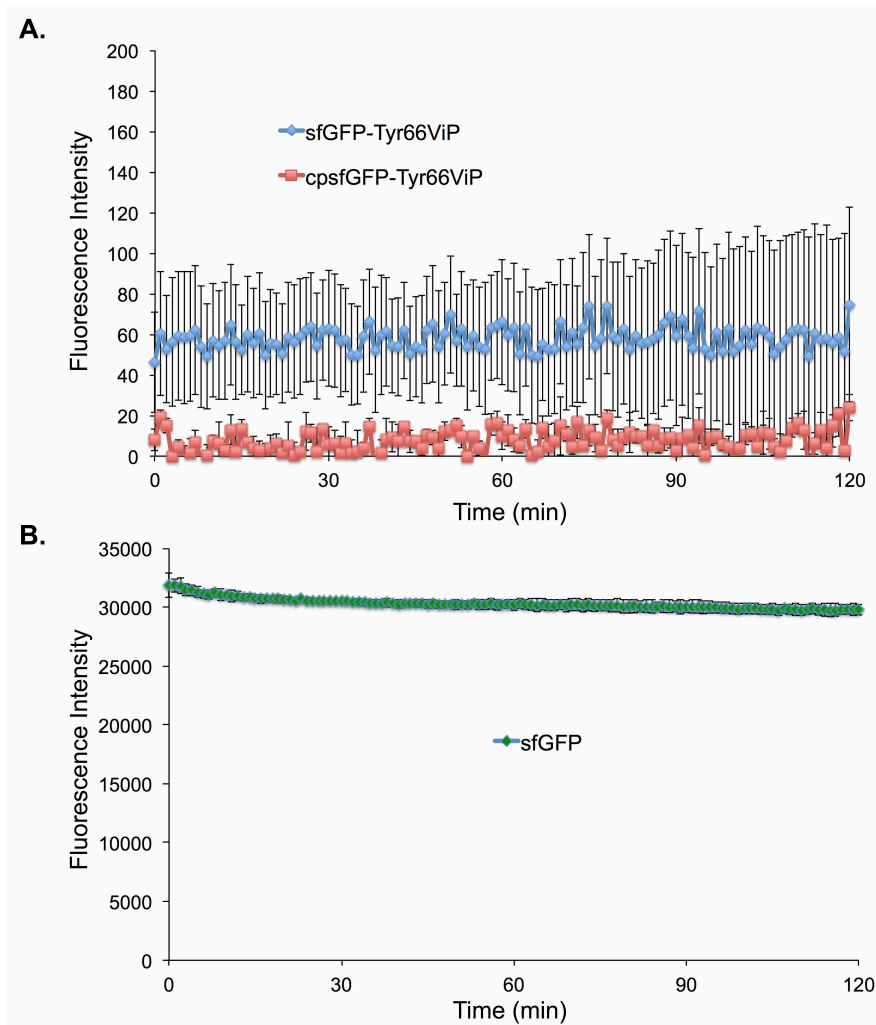


Figure S11. Photostability of the probes. (A) Protein samples ($0.5 \mu\text{M}$), sfGFP-Tyr66ViP and cpsfGFP-Tyr66ViP, were irradiated at 485 nm and the fluorescence signals were detected at 513 nm; (B) As a comparison, the fluorescence intensity of sfGFP ($0.5 \mu\text{M}$) was $\sim 30,000$.

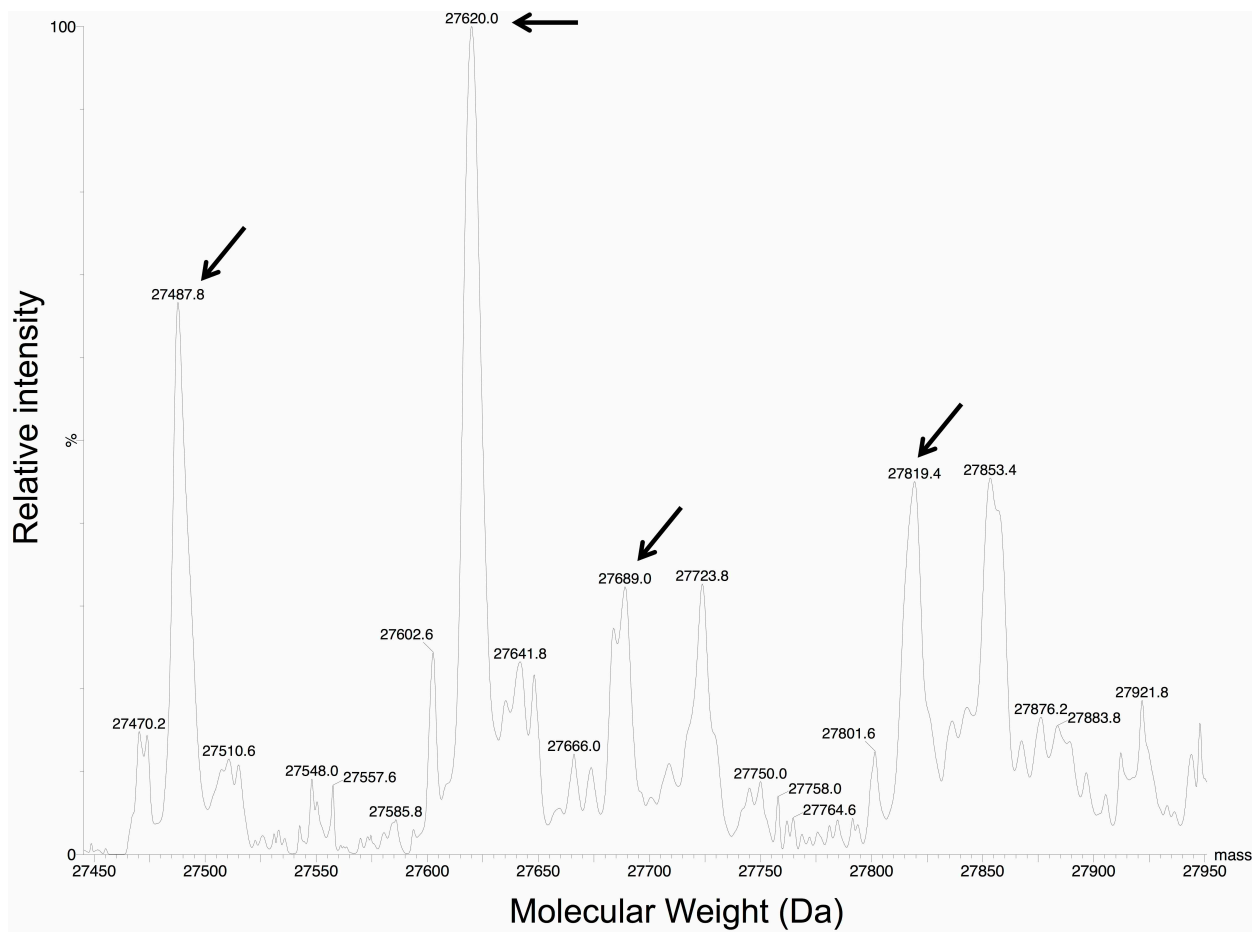


Figure S12. Mass spectrometry analysis of the deprotection of sfGFP-Tyr66ViP with Hg^{2+} .

This is deconvoluted ESI-MS spectra of the sfGFP-Tyr66ViP after the treatment with 100 μM Hg^{2+} . Expected masses: 27490.1 Da ($M + \text{Hg}^{2+}$; without the N-terminal Met), 27621.2 Da ($M + \text{Hg}^{2+}$; with the N-terminal Met), 27690.7 Da ($M + 2\text{Hg}^{2+}$; without the N-terminal Met), and 27821.8 Da ($M + 2\text{Hg}^{2+}$; with the N-terminal Met); observed masses: 27487.8 Da ($M + \text{Hg}^{2+}$; without the N-terminal Met), 27620.0 Da ($M + \text{Hg}^{2+}$; with the N-terminal Met), 27689.0 Da ($M + 2\text{Hg}^{2+}$; without the N-terminal Met), and 27819.4 Da ($M + 2\text{Hg}^{2+}$; with the N-terminal Met). There were no obvious signals corresponding to sfGFP-Tyr66ViP, which indicated a complete deprotection.

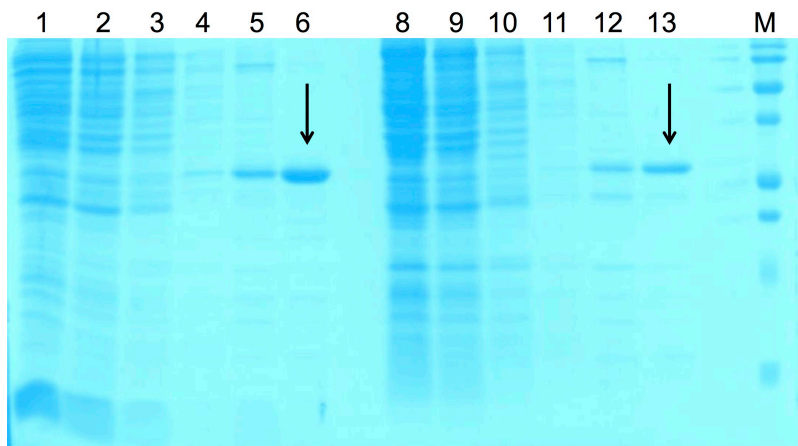


Figure S13. SDS-PAGE analysis of purification of sfGFP-Tyr66ViP and cpsfGFP-Tyr66ViP. Lane M, molecular weight marker; Lane 1-6, purification of sfGFP-Tyr66ViP; Lane 8-13, purification of sfGFP-Tyr66ViP; Lane 1 and 8, cell lysate; Lane 2 and 9, pass through fraction; Lane 3 and 10, first wash fraction; Lane 4 and 11; second wash fraction; Lane 5 and 12, first elution fraction; Lane 6 and 13, second elution fraction. The protein purity was estimated based on the second elution fractions (arrows). The second elution fractions were used for sensor characterizations.

Table S1. Calculation of quantum yield (ϕ).

	fluorescein	sfGFP-Tyr66ViP	cpsfGFP-Tyr66rViP
490	23876.0345	2933.65469	1244.56582
491	26888.74748	3097.91937	1276.11121
492	31749.26281	3649.55827	1326.34144
493	37302.852	3876.83561	1047.60833
494	44787.72369	4456.22539	1028.04536
495	51590.8316	4313.70009	1234.71991
496	56535.83891	5191.12924	998.56232
497	64566.34103	5768.35184	1131.34141
498	73281.45709	6386.55865	998.54047
499	78796.85318	6597.74183	1308.32441
500	89231.64885	6837.80331	938.05193
501	95930.21524	8176.21529	1101.7519
502	104434.3492	8697.09269	1090.80788
503	110874.3546	8776.42456	1286.94997
504	118088.4859	9529.05907	1256.98665
505	124163.9683	9744.39411	1504.0615
506	130623.0561	9709.18455	1430.03295
507	134629.1726	10742.30971	1296.78039
508	138606.1214	10406.90279	1297.98378
509	139235.44	9803.90239	1433.24853
510	142214.8967	10667.46626	1318.2265
511	142965.6054	10616.91446	1390.14025
512	144605.4251	10226.29883	1493.1432
513	143223.9997	10376.02846	1370.37779
514	140021.2229	9434.25405	1235.28403
515	142867.1915	9344.87047	1450.58823
516	137812.4872	9116.23098	1234.73508
517	136424.1237	8214.99595	1256.93685
518	130950.4546	8136.59495	1494.24722
519	129094.113	7829.33432	1369.12609
520	124944.8702	7864.95935	1235.41749
521	121892.7607	7025.81436	1195.27061
522	118868.8343	7064.51443	1020.51377
523	113182.053	6225.21883	1040.04651
524	109169.9044	5407.01895	977.44974
525	103003.2126	6237.96309	1080.87654
526	100082.2676	5413.42326	1174.28694
527	96797.55017	5086.9111	1081.39363
528	90855.18232	5120.07667	895.2911
529	89006.36249	4731.59424	1225.11766
530	85129.23076	4714.04399	855.16733
531	79834.34204	4391.13978	1185.97031
532	77803.90893	4603.74125	957.93509

533	73316.82299	4216.3082	875.09447
534	70501.25655	4569.23661	1060.67072
535	67499.13336	4087.90008	1030.24785
536	66014.32907	3794.71394	1030.00728
537	62832.59871	3774.27979	987.59581
538	60166.33976	3754.21055	1122.07758
539	57332.26315	3921.22198	844.79432
540	54595.12115	3566.87544	1134.17934
541	55556.76939	3515.69386	1183.76542
542	51004.0065	3680.74416	834.12616
543	50351.01486	3396.27497	1071.64684
544	49263.22683	3406.05941	834.99376
545	47166.37625	3342.29556	998.57616
546	47007.04313	3352.20957	905.2345
547	44702.32045	3087.81106	966.86718
548	43190.60873	3201.2512	1132.99422
549	42709.22703	3022.35866	917.05833
550	40909.30827	2918.55426	895.88198
551	38564.17088	2642.49988	885.50655
552	37838.61646	2726.82309	906.67333
553	36709.37395	2766.6228	855.58623
554	38212.5139	2281.44662	1009.15168
555	34263.22576	2426.97897	1049.65508
556	34278.38127	2172.16779	1049.96484
557	32226.09003	2377.83595	855.01539
558	31164.101	2106.59441	741.30089
559	30026.89314	1808.89724	864.50222
560	28791.82322	2190.94967	864.71445
561	27920.70652	1810.86304	896.44905
562	26669.26749	1788.96374	834.81218
563	25635.95963	2013.74064	813.4007
564	24445.26645	1810.12966	957.37591
565	24246.8882	1647.19308	823.81403
566	22356.4911	1605.90006	783.01853
567	22054.90308	1603.48117	834.21683
568	21758.92054	1634.48742	750.90518
569	20383.5004	1491.6986	751.35344
570	19041.75673	1656.86222	741.61485
571	18982.15518	1376.9052	824.42456
572	16929.62218	1491.00808	812.88703
573	17081.5156	1264.81252	751.78871
574	16496.13811	1533.83053	937.77498
575	15768.3831	1542.1756	752.38505
576	14690.0035	1418.81083	906.00555
577	14529.20345	1398.53149	740.8559
578	12937.7598	1389.84498	843.6332

579	12994.21223	1214.37053	813.6072
580	12342.11715	914.23094	793.02727
581	11227.06436	1243.43687	967.25969
582	10974.66784	997.92589	772.04486
583	10753.33063	1183.86462	948.00178
584	10202.79689	1038.7384	804.26153
585	9826.33928	1120.50955	937.19672
586	9123.3629	967.02595	710.28957
587	9107.48423	1224.85195	885.51812
588	8507.31947	1131.53611	742.04388
589	8678.52423	1057.79226	761.62481
590	7598.40068	1047.96996	833.61114
591	7354.65325	966.5488	627.76485
592	7331.21059	1069.7153	741.73871
593	7146.41591	945.43684	762.3683
594	6712.6969	1079.44967	895.55973
595	6785.77272	1007.75497	720.46612
596	6287.39208	1039.51928	916.87527
597	5876.82575	1120.81114	782.95922
598	6502.48336	1017.13401	885.2904
599	5903.19968	1058.53606	915.44662
600	5715.99751	771.58973	740.80728
601	5102.64737	998.22631	792.89978
602	5296.56276	986.26437	762.12629
603	5057.59882	843.03202	802.59282
604	4867.70897	1152.15544	689.70078
605	4977.34624	1132.37299	690.26764
606	4928.45412	1089.81244	875.88254
607	4574.19153	1068.87156	803.10336
608	4070.93272	863.52572	740.60677
609	3968.83032	854.0292	771.79036
610	3801.50833	730.12148	957.46945
611	3938.34926	965.47454	782.54896
612	3972.23745	945.53821	678.64432
613	3504.18351	843.80834	668.92969
614	3746.83412	844.23154	793.03694
615	3210.92091	822.93193	587.4474
616	3247.23231	832.81835	761.70958
617	3120.33478	668.36608	689.6379
618	3075.07526	915.60057	916.24773
619	3285.73076	832.9177	834.21855
620	2866.20026	934.66361	792.63451
621	2518.61522	822.10658	709.69188
622	2947.04822	925.69	781.88324
623	2304.70143	833.5922	772.38122
624	2379.46643	894.42727	813.80694

625	2540.09524	853.43819	906.05028
626	2464.59916	823.15865	1049.6619
627	2390.03904	915.77788	679.81158
628	2084.72508	904.76825	710.95356
629	2002.26626	780.65321	669.38996
630	2075.82636	760.5977	946.54222
631	2010.63121	709.6487	792.04798
632	1620.8102	1039.12025	772.1581
633	1948.42139	791.23018	854.43799
634	2002.38514	822.61926	966.99915
635	1801.34706	1038.97199	853.89806
636	1925.91127	802.72189	710.41774
637	1580.35592	688.61903	762.49364
638	1602.70756	739.58972	782.74825
639	1582.16459	852.56604	761.37899
640	1578.92357	853.47037	874.93859
641	1726.64705	699.31407	751.63824
642	1485.30341	934.85608	823.51586
643	1443.52469	894.28869	853.18792
644	1431.1452	750.91533	884.53934
645	1684.66912	751.22595	679.64317
646	1221.46199	914.6466	762.51719
647	1571.06315	873.37727	771.96637
648	1380.60009	750.15423	700.02185
649	1537.44712	709.67958	700.25888
650	1316.65999	698.76582	710.6545
651	1138.51833	904.42225	772.13898
652	1148.90155	791.54925	781.50736
653	1115.4965	802.72216	750.98424
654	1105.09793	802.65169	792.69627
655	1053.2068	750.64146	720.95283
656	1390.98784	822.46721	771.53445
657	1147.40547	740.58465	864.47406
658	1105.42399	884.79227	576.58961
659	1000.50422	760.49617	680.00218
660	1170.51749	678.04325	823.26458
661	1127.62465	781.2397	637.86027
662	1010.52956	843.51689	658.40389
663	1189.24966	792.10484	792.8315
664	1158.74622	894.35077	813.26298
665	863.99762	915.12661	699.41226
666	978.68222	751.09043	895.19956
667	820.57629	740.8531	854.68495
668	842.53051	729.50919	711.07251
669	885.71542	842.53495	740.91624
670	1106.56006	729.78702	669.02179

671	958.2119	843.56049	751.45146
672	768.63173	781.76608	741.5288
673	958.83678	740.21729	658.40757
674	1116.74358	771.20253	761.01316
675	957.46749	905.76347	719.82886
676	1146.89222	689.64058	885.5548
677	800.31989	719.39101	761.9379
678	853.62003	729.62153	792.39007
679	863.12197	812.50493	648.38697
680	884.19531	833.40558	710.69721
681	1063.61823	760.44355	772.46007
682	1001.48329	883.7965	967.09957
683	1074.66063	822.52631	791.84313
684	999.41445	833.84469	997.77851
685	831.56758	803.02049	895.78612
686	695.45137	657.94297	761.42282
687	927.31477	750.73872	812.58001
688	757.49578	771.57755	678.91271
689	999.8856	956.88232	865.15284
690	905.83294	688.27161	896.01833
691	695.75207	883.79953	813.3511
692	715.98822	750.89175	812.76476
693	957.90238	885.3778	679.10418
694	926.2972	864.38645	792.68851
695	779.45805	843.23173	658.57744
696	1032.27855	915.20557	771.37617
697	873.06116	740.81807	534.88519
698	894.46902	966.90002	844.48456
699	821.40385	862.96483	793.18876
700	853.6715	883.86358	679.24722
Area	6387788.86	489505.9283	150591.8494
Abs	0.051	0.05	0.047
ϕ	0.925	0.072301833	0.023662736

IV References

- (1) Rudolf, J. D.; Poulter, C. D. Tyrosine O-Prenyltransferase SirD Catalyzes S-, C-, and N-Prenylations on Tyrosine and Tryptophan Derivatives. *ACS Chem. Biol.* **2013**, *8*, 2707-2714.